Influence of laser spatial parameters and illuminator pupil–fill performance on the lithographic performance of a scanner

Stephen P. Renwick[a*], Steven D. Slonaker[a], Ivan Lalovic[b**], and Khurshid Ahmed[b]
[a]Nikon Precision, Inc., 1399 Shoreway Road, Belmont, CA 94066
[b]Cymer, Inc., 16750 Via Del Campo Court, San Diego, CA 92127

ABSTRACT

Litho–tool illuminator performance, characterized by quantitative measurements of pupil–fill intensity distribution and cross–field uniformity, has been cited as a key contributor to CD uniformity. While both modeling exercises with simulated pupil fills and measurements of real pupil fills have been undertaken, quantitative assessments of the pupil's effect when compared with other CD error contributors are rare.

An integral part of illuminator performance is, of course, the laser. Not only must a litho laser meet stringent requirements at installation, but also the litho tool and laser suppliers are responsible for ensuring performance after maintenance activity, such as laser module replacement.

We have investigated the effects of adjustable spatial laser parameters on the illuminator pupil fill as measured via a pinhole reticle and on illumination uniformity as measured by the scanner. We present the experimental results of these studies, estimates of their effects on litho performance via modeling, the sensitivity of lithographic performance to the spatial parameters, and an assessment of their importance relative to other lithographic variables affecting CD uniformity.

Results show that not only is the baseline illuminator pupil–fill performance a small contributor to lithographic error, but also that the system is stable in the presence of laser adjustments.

Keywords: laser, illuminator, pinhole, pupil, pupilgram, CD uniformity, CD control, linewidth abnormality

1. INTRODUCTION

When thinking about contributors to less–than–perfect lithographic tool performance, the list of prime suspects is frequently topped by the lens and closely followed by the tool's focusing system and stages. Lens aberrations cause errors including CD non–uniformity and linewidth abnormality (LWA) while focusing errors reduce CD performance and stage synchronization errors can reduce image contrast.

A less–frequent suspect, but one which gets occasional press, is the performance of the litho tool's illuminator. This is most frequently mentioned in the context of providing (or failing to provide) isotropic illumination along the lighted slot of a scanner. Because resist CD changes with dose, non–uniformity in the power delivered to the slot can be a significant contributor to CD non–uniformity [1]. For that reason, scanner manufacturers provide means for both measuring and adjusting power uniformity.

In addition to providing uniform illumination power, though, the illuminator is also required to deliver a certain pupil fill or angular distribution of light impinging on the reticle. Actually it needs typically to deliver several options: circular, annular, quadrupole, etc. Clearly one would want the pupil fill to be uniform along the slot, and one would expect the actual pupil fill pattern to closely resemble the ideal case seen in textbooks or used in CD modeling calculations. This has received some attention in recent years, with work being published concerning quantification of condenser errors [2], the estimated effects of pupil–fill errors [3], trial limits on pupil–fill aberrations [4], and a means of measuring the pupil fill through generation of an intensity plot called a "pupilgram" [5].

* contact author: srenwick@nikon.com
** Present address: Advanced Micro Devices, Sunnyvale, CA

Optical Microlithography XV, Anthony Yen, Editor, Proceedings of SPIE Vol. 4691 (2002) © 2002 SPIE · 0277-786X/02/$15.00

While this has all been valuable, little work has been done to determine the importance of pupil−fill errors relative to the other imperfections in a scanner. Suppose that a user has a set of pupilgrams in hand; one would like to know if the imperfection observed is an important or a minor effect. Additionally, it would be nice to know how stable the pupil−fill performance of a scanner is. After all, in the normal course of events, lenses are replaced, optics are adjusted, and lasers are serviced. A system should be stable in the presence of these adjustments.

In this study, we have measured pupilgrams for different Nikon scanners both under normal operating conditions and with deliberate misadjustments introduced to the laser. We have taken the pupilgram data and fit them to appropriate basis functions in order to parametrize their behavior, and then analyzed the modeled response of isolated and dense lines to the basis functions in order to extract expected lithographic effects of imperfect pupilgrams. This allows us to place bounds on the relative importance of imperfections in the pupil fill and show that normal adjustments to a scanner will not significantly detract from its performance in this area.

2. EXPERIMENTAL METHOD

2.1. Principle of operation

We generate 3−D plots or contour plots of the intensity as a function of angle of the light impinging on the reticle plane. This is called a pupilgram. A plot of a perfect circular pupil fill would be round, would have a diameter corresponding to the partial coherence value (sigma) selected, and would be flat across the top, indicating perfectly uniform angular intensity. Similarly, a perfect annular pupil fill would look like a ring and a perfect quadrupole would look like four pillars.

Pupilgrams are generated by use of a pinhole reticle, a means of photographing images on a wafer through an optical microscope, and appropriate software to analyze the images. The method was clearly described by Kirk and Progler [5], so we give a brief outline here.

The pupil fill describes the angular distribution of light impinging on the reticle. We want to transform this into a spatial distribution at the wafer plane. The measurement employs a pinhole camera at the reticle plane. A small hole, on the order of 50 microns diameter, is placed close to but not coincident with the reticle plane. Kirk’s measurement used a reticle with a pinhole in the chrome inserted upside down, so that the chrome side was one reticle thickness away from the reticle plane. In this study, we employed a commercial reticle, the Litel SMI (Source Measurement Instrument), which uses a thin metal plate, with pinholes punched in it, at the pellicle plane. There is no pattern on the SMI reticle in the region immediately above the pinholes. Details of the Litel reticle and its use have been described by Farrar and co−workers [6]; our use is similar except that we did not employ Litel software.

Figure 1 shows the basic geometry. For this application, bear in mind that the lens here functions solely to transfer the reticle−plane pattern to the wafer plane. For that reason, the figure is drawn as if the lens didn’t exist.

Consider two light angles incident on the reticle, θ_1 and θ_2. For each reticle point, the pinhole allows only light from one angle to pass through and hit the wafer. Thus, light incident at angle θ_1 strikes the wafer only at point x_1, while light incident at θ_2 strikes the wafer only at point x_2. Any angle−dependent intensity variation between angles θ_1 and θ_2 will be seen as a spatial variation between x_1 and x_2. Note that the two rays come from different spots on the reticle plane; use of the device requires spatial variation in pupil−fill pattern between those two points to be small. That requirement is usually met.

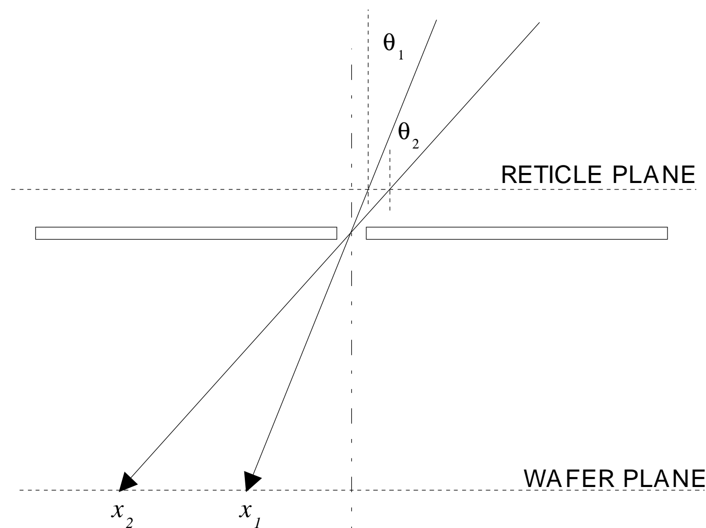

Figure 1.
Basic operation of the pinhole camera.

A single pinhole thus will project a pattern of the pupil fill intensity, or the degree to which it approximates the angular intensity distribution intended by the illuminator designers. An array of pinholes in the illuminated field will yield several patterns, allowing the user to see the pupil–fill uniformity, or the difference between the pupil fills visible at different points in the field.

2.2. Procedure

This particular reticle has 45 points available for measurement of pupilgrams at different points in the field, and employs an exposure of numbered frames to, among other things, identify positions in the field for the user. In all measurements reported here, we used field points #19 through #27, which range along the center of the slot parallel to the long axis. Site #23 is the center of the field.

Now, the intensity in the aerial image as a function of radius is directly proportional to intensity as a function of angle. This is not true of the exposed image, since the resist response is nonlinear. Therefore we use Kirk's method of dose–to–clear contours to remove the nonlinearity.

A series of exposures is made, increasing dose each time, such that in the first one the resist begins to clear in the center of the pattern and in the last one resist has cleared at the edges. In each exposure, then, we know exactly what the dose was in the threshold region (and only in the threshold region). The dose–to–clear threshold in each exposure thus represents a single contour through the real intensity distribution.

The exposed images are quite large, on the order of 200 μ diameter. They are thus easily visible with an optical microscope. We used a microscope with CCD camera to produce digitized grayscale images which were fed to analysis software that produced pupilgrams. Sample photos are shown in figure 2. The flyseye elements in the Nikon illuminator are clearly visible in all pictures. We can also see the dose–to–clear threshold in the center of the first picture spreading out in the second one.

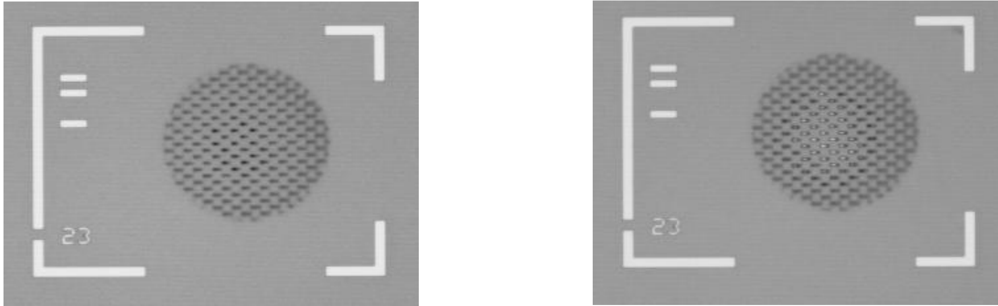

Figure 2.
Digital photographs of pinhole exposure from a Nikon S202.
The darkest spots are the dose–to–clear threshold. The white spots are where resist has cleared.

Software was written to analyze the grayscale digital photos. For each picture, the dose–to–clear threshold area is identified via grayscale level. Pixels thus identified are assigned a numerical value of the reciprocal of the dose for that picture, while others are assigned zero. Each picture thus forms a single intensity contour, and the set of contours from the set of pictures is assembled to form a single contour map.

Additional work is done to improve pupilgram readability. The software has an adjustable "blob factor" which dithers the individual flyseye elements to merge them together. This makes the picture smoother but also introduces a blocky quality as a processing artifact. It can at times tend to magnify irregularities near the edge of the pupilgram. Partially due to these processing artifacts, we decided to extract most of the quantitative information not from raw pupilgrams but rather from fits of basis functions to them; this is discussed in a later section.

A sample pupilgram, produced by our analysis software from photos taken from a Nikon S202, is shown in Figure 3. Note that gray scale on the pupilgram was selected such that the black part corresponds to intensity 0.60; i.e. the pupilgram deliberately emphasizes variation at the top. We see that the intensity profile is "hot" in the center and tapers more or less smoothly to the edges. Irregularity in the perimeter is seen, some of which is due to the processing and some of which is real (compare the pupilgram to the wafer photos). The peak intensity is slightly offset from the center of the pupil.

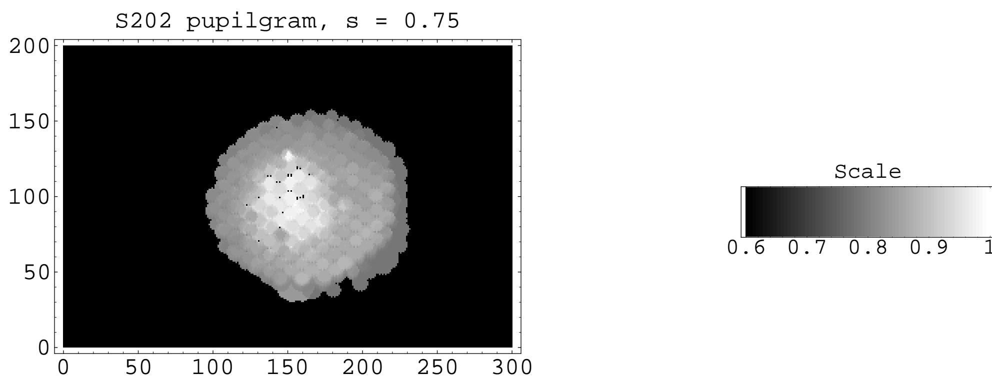

Figure 3.
A sample pupilgram, taken at large partial coherence, from a 0.60–NA KrF scanner.
Scale indicates intensity, normalized to the peak value.

We should mention, by the way, that the scanners used in this study are training tools, and hence do not represent the quality of Nikon illuminators in general. We deliberately wished to use sample scanners likely to have sub–par performance.

2.3. Measurement quality

Performing measurements is not useful if you don't know how good the measurement tool is. Thus, prior to using the system to make actual judgments of illuminator and laser performance, we decided to evaluate its precision. A simple test, obviously, was a repeated measurement on the same tool with the same partial coherence settings. We also performed exposures using knowledge of the details of the illuminator to inspect for improper differences in intensity distribution from one setting to the next.

These tests showed that:

- Measurement of partial coherence simply by measuring the diameter of the exposed circle is accurate to ±0.05.
- The tool does not allow the user to compare intensity measurements from one point in the slot to another. They must be normalized to each other. We speculate that this is due to differing size of the pinholes in the plate. Presumably a reticle could be carefully constructed to minimize this effect.
- If peak intensity values are normalized to each other, the intensity profile in repeated measurements is repeatable to about ±5%.

Presumably one could make an effort to track down sources of error in this measurement, whether they come from the reticle or from the litho tool. In any case, though, the measurement is certainly good enough for our purposes.

3. MEASUREMENTS AND ANALYSIS

3.1. Baseline equipment settings

The effective dose at the wafer plane is reduced by the pinhole camera's diffuse image. Effective dose D_{eff} is related to the nominal dose D_{nom} by the ratio of pinhole area to pattern area:

$$D_{eff} = \frac{A_{pattern}}{A_{pinhole}} D_{nom} \quad . \tag{1}$$

Therefore, very high doses are needed for exposure. In this study, doses ranging from around 1500 to 5000 mJ/cm^2 were used.

Exposures in this set were shot with a Nikon S203 KrF scanner, with the lens NA set to 0.68 and the partial coherence set to circular illumination, with $\sigma = 0.40$.

A sample of three pupilgrams, from sites 19, 23, and 27, is shown below. Individual flyseye elements are clearly visible.

Comparing sites 23 and 27, it is clear that again, the pupilgrams tend to be more intense in the center with some drop–off toward the edge. Minor variation is seen from one point to the next. Site 19 is distinct from the rest, and its pupilgram indicates a possible defect in this particular illuminator (again, we emphasize that this is not a typical Nikon scanner). This particular tool then is an extremely instructive case for analyzing pupil effects.

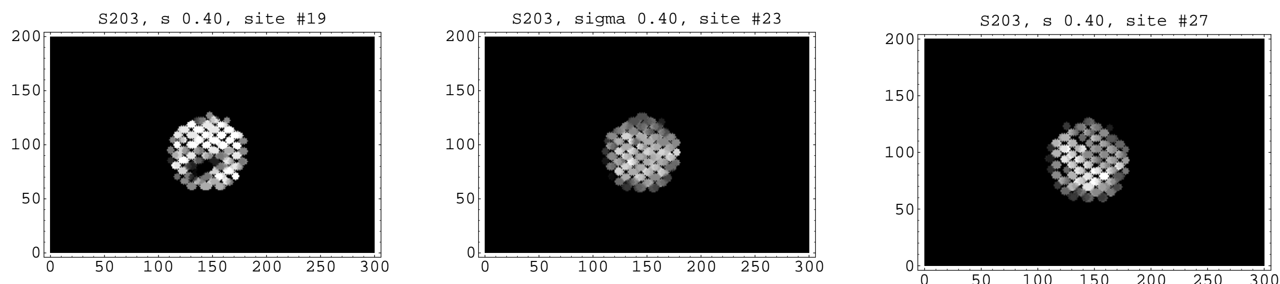

Figure 4.
Several pupilgrams from different points in the slot of a Nikon S203 scanner

3.2. Misalignment of laser beam

Now we have a good idea of the baseline performance of the tool, although we have yet to calculate whether the imperfections seen are important. Next we introduce a deliberate misadjustment into the optics in order to see the effect.

We wanted to emulate a misadjustment that could conceivably occur during initial laser installation or during periodic maintenance, such as laser chamber replacement. Accordingly we deliberately set the *pointing* of the laser beam away from its nominal value. A wedge optic was inserted into the excimer laser path such that the beam was deflected by 2.5 mrad, an angle significant when compared with normal installation and adjustment tolerances.

Effects of this misadjustment were not especially large but were readily visible. Rotating the wedge optic, thus sweeping the incident beam about in a narrow cone, changed illumination power by -15% to + 6% (showing that this training scanner may well not have been optimized at the start). Power uniformity varied by -0.3% to +0.1%. When the wedge was removed, power and uniformity readings returned to their previous values with negligible error. Maximum beam power and best uniformity did not occur at the same wedge rotation angle.

One might expect that we should then have picked the worst power/uniformity combination and remeasured the pupil fill. This would not have been especially useful, though, since nobody would willingly adjust a tool that way. Rather, since the goal was to search for *unsuspected* degradation in pupil–fill performance while adjusting the illuminator/laser combination, we picked a wedge–optic setting that improved power and did not change uniformity.

We then exposed a wafer with the pinhole reticle using the same illumination settings. Results are shown in Figure 5. Qualitative changes in the pupilgram are definitely visible. Generally, intensity seems to have shifted toward the $+y$ direction.

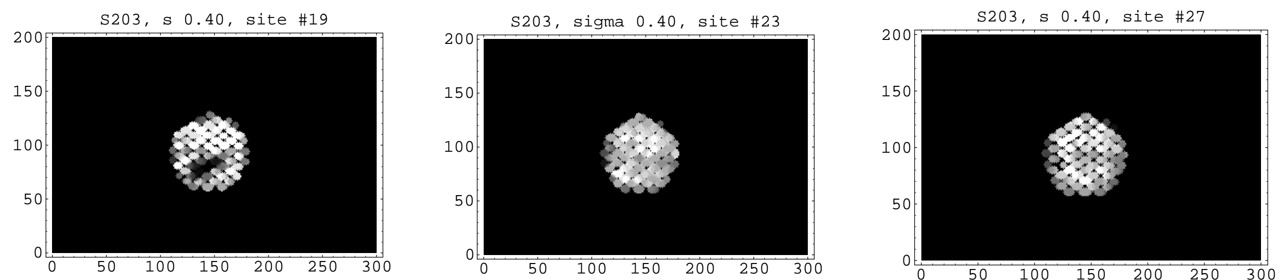

Figure 5.
Pupilgrams from the same locations on the same tool as Figure 4, with the laser beam pointing shifted.

3.3. Analysis of pupilgrams: curvature & tilt

In order to make sense of the different pupilgram results, we need to find common basis functions capturing their behavior. An obvious candidate would be Zernike polynomials, but these are sufficiently complicated that such an analysis might obscure physical effects. Fits using the basis functions suggested by Barrett [4] were intractable due to the functions' discontinuous behavior.

Inspection of the pupilgrams observed so far revealed certain key features. They tend to be more intense in the center. Some, especially site #19, show a distinct tilt or asymmetry in *x* or *y*. Basis functions should at a minimum account for the following qualitative features:

- Intensity maxima or minima ("dome" or "dish").
- Asymmetry in the intensity in the *x* or y directions.
- Overall tilt in *x* and *y*.
- Location of the peak intensity away from the geometric center of the pupilgram.

Polynomial functions in *x* and *y* can reproduce these qualities. Defining the point ($x = 0$, $y = 0$) as the geometric center of the pupilgram, data were fit, using a linear least–squares fit, to the function

$$f(x) = a_1 x^2 + a_2 y^2 + a_3 y^2 + a_4 x + a_5 y + a_6 \quad \cdot \tag{2}$$

As a criterion of goodness of fit, we used the reduced χ^2 parameter, which compares deviation from fit to experimental error [7]. An ideal fit has $\chi^2 = 1$. This parameter was rather variable, ranging from about 0.5 to 1.5, indicating that this choice of fitting function captures the features in the data reasonably well. Inclusion of higher–order terms did not improve the goodness of fit as described by χ^2. The power center, defined as the expectation value of the pupilgram in *x* and *y*, generally was only insignificantly different from the geometric center.

The fit returns six fit coefficients, which have little intuitive physical meaning. Thus, with some additional calculation, all our pupilgrams are described in terms of *curvature* and *tilt* in the *x* and *y* directions. These parameters range between 0 and 1, such that:

- curvature (*x* or y) is the fractional drop from peak to edge of the pupilgram, i.e. "20% curvature" means that intensity at the edge is $0.8 \times$ the peak intensity;
- tilt (*x* or *y*) similarly describes drop in intensity from one side to another.

Samples of idealized pupil fills with 0.30 curvature and tilt, respectively, are shown in Figure 6.

Figure 7 shows results of analyzing all the pupilgrams collected. Curvature and tilt parameters are plotted as a function of slot position for wafers exposed at baseline setting and with the beam misadjustment introduced. Both parameters tend to be constant along the slot. We may expect, then, that this behavior would induce an overall shift in some lithographic parameter relative to another tool, and that we should therefore expect effects to show themselves in lithographic parameters such as CD uniformity and LWA uniformity along the slot. We might also expect an HV bias effect from differing *x* and *y* behavior seen.

We see that the pupilgrams change when the incident laser beam is deflected, as shown in the lower two graphs. Overall curvature has actually lessened, but the variation in curvature along the slot has increased. We might expect this to affect CD uniformity. Performance as measured by tilt of the pupilgram actually seems to have improved somewhat.

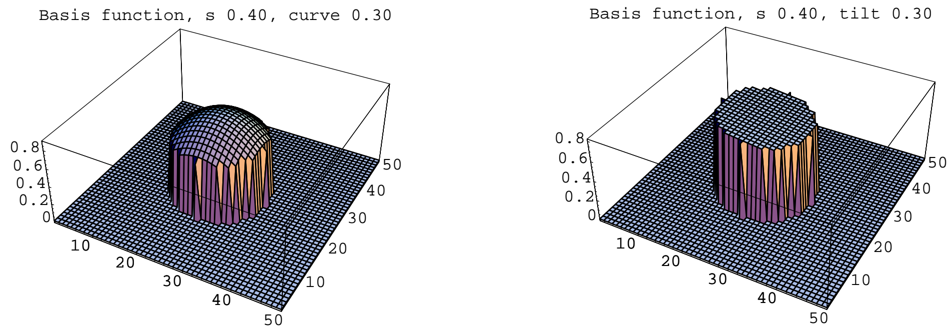

Figure 6.
Idealized pupil fills used as basis functions for fits to data.

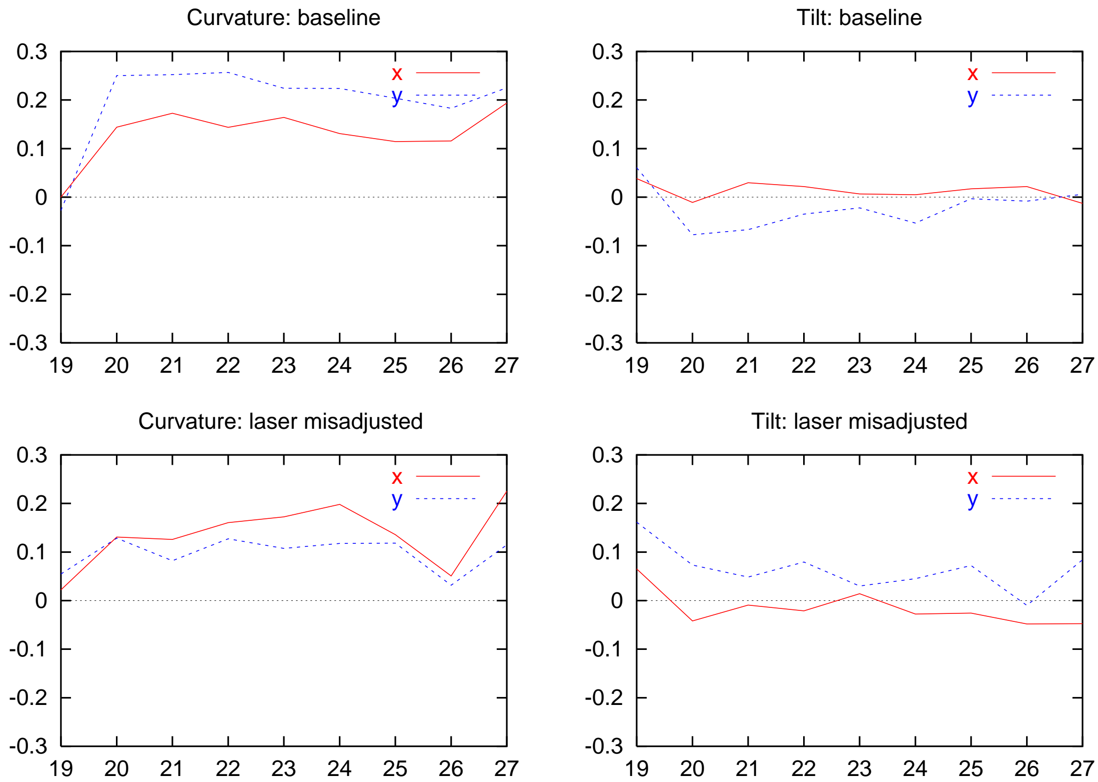

Figure 7.
Summarized results of pupilgram analysis in terms of basis functions.

4. CONNECTION TO LITHOGRAPHY

4.1. Sensitivity

Now that we have quantified the pupilgram performance, we need to figure out what it means in terms of lithographic effects. To that end, aerial image calculations were performed using Prolith, which allows the user not only to select an illumination pattern (standard, annular, quadrupole) but also to employ user−generated files describing custom pupil fills.

Initially the plan was to feed the experimental pupilgram files directly into Prolith. Doing that might have allowed the details to obscure the underlying patterns of behavior, though. In order to spot trends occurring in the lithography as pupilgrams change, then, a series of idealized pupil fills based on curvature and tilt parameters was used. Aerial−image calculations were run for 150−nm isolated lines and 180−nm grouped lines exposed with 248−nm light, with a NA of 0.68, separately with idealized pupil fills with curvatures of 0.10, 0.20, 0.30, and 0.40 and with tilts of 0.10, 0.20, 0.30, and 0.40. The idealized functions used has integrated intensity normalized in order that each modeling run had the same dose. In order to check for dependence on partial coherence, calculations were run with partial coherence (σ) values of 0.4 and 0.7.

Parameters analyzed from the aerial−image output included CD through focus for both isolated and grouped lines as well as linewidth abnormality (LWA) for a 5−line group. In all cases, CD was determined by finding an aerial−image threshold value that yielded the nominal line size at best focus. In this fashion we are able to assess the pupil fill effects on CD uniformity, HV bias, and LWA.

Results showed:

- Isolated−line CD through focus was sensitive to curvature.
- Grouped−line LWA was sensitive to tilt, but only through focus; LWA at best focus was unchanged.
- These were the only sensitivities found.
- The effects seen were much larger at $\sigma = 0.7$ than at $\sigma = 0.4$.

The results of the analysis are shown graphically in Figures 8 and 9. From these, we can obtain sensitivity parameters ΔCD/Δcurvature and ΔLWA/Δtilt. Note that the CD uniformity effect on isolated lines is strongest at best focus.

	ΔCD/Δcurvature, @ best focus	ΔLWA/Δtilt, @ 0.3 μ defocus
$\sigma = 0.4$	0.2 nm per 10% curv.	0.002 per 10% tilt
$\sigma = 0.7$	1.2	0.010

Table 1.
Parameters for lithographic sensitivity to pupil−fill imperfections, found by aerial−image modeling

While neither of these effects is particularly sensitive, this does show that we can observe both CD uniformity and coma−like LWA effects that have nothing to do with the lens.

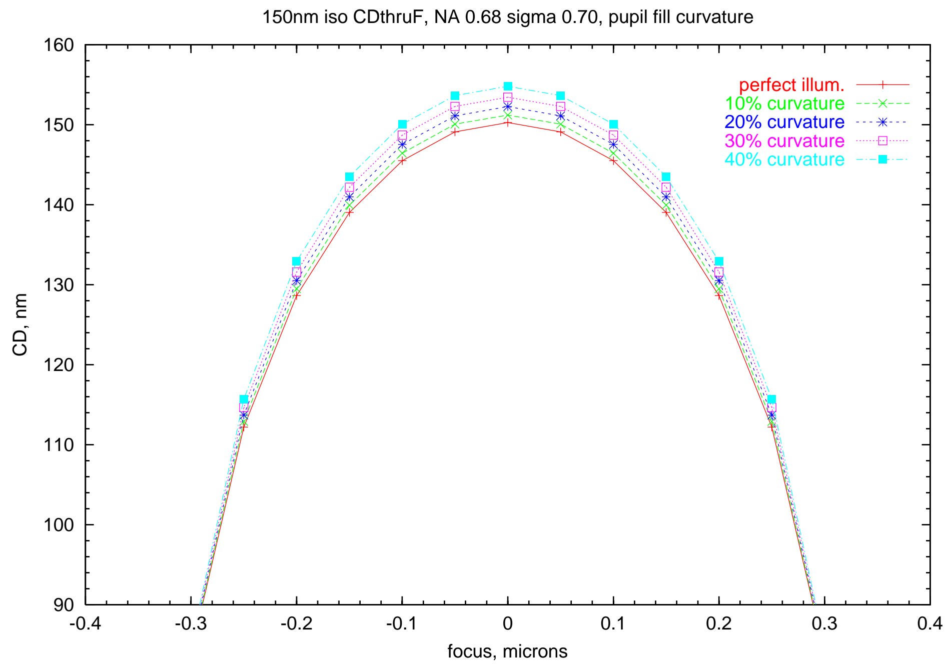

Figure 8.
Sensitivity of isolated–line CD through focus to changes in pupil–fill curvature.

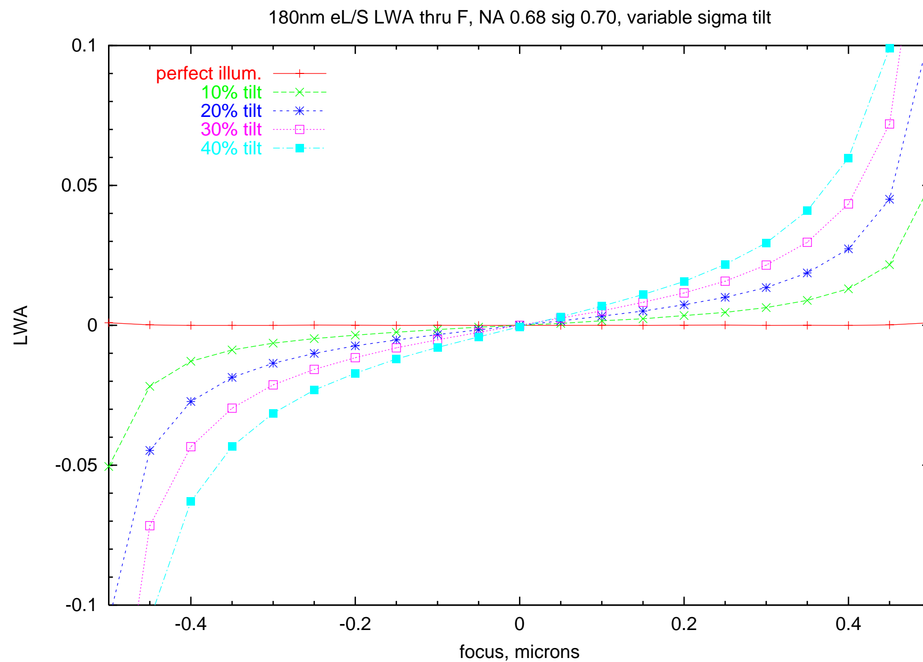

Figure 9.
Response of linewidth abnormality to changes in pupil–fill tilt.

4.2. Results

Now we can connect the pupilgram data to the sensitivity calculation and estimate the effects on lithography. Since the effects at $\sigma = 0.4$ are so small, we include estimated effects at $\sigma = 0.7$, even though the test exposures were shot at $\sigma = 0.4$.

Condition	Curvature slot TIR	CD TIR, $\sigma = 0.4$	CD TIR, $\sigma = 0.7$
Baseline, exclude site #19	0.05	0.1 nm	0.6 nm
Baseline, include site #19	0.20	0.4	2.4
Beam misadjusted, exclude site #19	0.12	0.2	1.4
Beam misadjusted, include site #19	0.12	0.2	1.4

Condition	Max. curvature $x - y$ difference	HV bias, $\sigma = 0.4$	HV bias, $\sigma = 0.7$
Baseline	0.11	0.2 nm	1.3 nm
Beam deflected	0.08	0.2	0.9

Tables 2a & 2b.
Effects of curvature in the pupil fill.

	Tilt variation TIR	LWA, $\sigma = 0.4$, @ 0.3 μ defocus	LWA, $\sigma = 0.7$, @ 0.3 μ defocus
Baseline, exclude site #19	0.07	0.001	0.007
Baseline, include site #19	0.15	0.003	0.014
Beam misadjusted, exclude site #19	0.07	0.001	0.007
Beam misadjusted, include site #19	0.15	0.003	0.014

Table 3.
Effects of tilt in the pupil fill

For CD uniformity, we immediately see that the illuminator can be expected to contribute a rather small effect. The largest effect is just over 2 nm with the anomalous point included. Under normal conditions, this effect is between 1 and 2 nm. When considered in the light of other contributors [1] to CD slot error, this is not an especially large contributor and is certainly not a driver.

Effects on LWA are practically within the noise level of LWA measurements. Recalling that LWA is defined as

$$LWA = \frac{L_1 - L_5}{L_1 + L_5} ; \quad (3)$$

an error of only ±2 nm in measurement of linewidth would induce a ±0.010 error in LWA, swamping most of the LWA effect seen here.

Moving the laser beam altered the signature of the illuminator effect. Actually the raw numbers indicate that CDU and LWA would improve as a result of this move, but this is mostly because the imperfection at point #19 did not stand

out as much from the rest of the slot. Other than that, we see that the effect of moving the laser beam is measurable but would have a small to negligible impact on CDU and LWA.

5. CONCLUSIONS

Our desire at the beginning of this study was to bound the problem: is pupil–fill performance a big contributor to scanner errors, or is it negligible? We also needed to find whether there were unexpected sensitivities to laser or illuminator adjustment: could good performance be unwittingly degraded? We clearly see these conclusions:

- Tilt errors, which could masquerade as coma or other lens–related effects, are almost certainly insignificant. It would take a truly gross illuminator defect to introduce enough linewidth abnormality even to be reliably measured.
- Variation in pupil–fill curvature has a nonzero contribution to but is not an important driver for slot–TIR CD error.
- Variation in pupil–fill curvature has a similar effect on HV bias.
- Both effects are much smaller at low partial coherence values.
- Adjustment of the laser pointing does not appear to be an issue. Results are visible in pupilgrams, but would have little measurable effect in lithography.
- There is no reason to suspect inadvertent degradation of litho tool performance due to laser pointing adjustment.

Pupilgrams produced by a pinhole reticle are an interesting diagnostic aid. They show results that cannot be seen any other way. Any results, though, must be carefully assessed in terms of their relatively small effects in the real world.

ACKNOWLEDGEMENTS

The authors express appreciation to I. Hikima and H. Kawai for valuable conversations, as well to R. Popescu and N. Farrar for supporting this work.

REFERENCES

1. S.P. Renwick and J.M. Brown, “Application of CD error budget analysis to ArF scanner performance,” *Optical Microlithography XIV*, C.J. Progler, ed., *Proceedings of SPIE* **4346**, p. 1587 – 1597, SPIE, Santa Clara, CA, 2001.
2. C. Krautschik, M. Shibuya, and K. Toh, “Mathematical treatment of condenser aberrations and their impact on linewidth control,” *Optical Microlithography XII*, L. Van den Hove, ed., *Proceedings of SPIE* **3679**, p. 87 – 98, SPIE, Santa Clara, CA, 1999.
3. Y. Borodovsky, “Impact of local partial coherence variation on exposure tool performance,” *Optical Microlithography VIII*, G. Fuller, ed., *Proceedings of SPIE* **2440**, p. 750 – 770, SPIE, Santa Clara, CA, 1995.
4. T.C. Barrett, “Impact of illumination pupil–fill variation on simulated imaging performance,” *Optical Microlithography XIII*, C.J. Progler, ed., *Proceedings of SPIE* **4000**, p. 804 – 817, SPIE, Santa Clara, CA, 2000.
5. J.P. Kirk and C.J. Progler, “Pupil illumination: in situ measurement of partial coherence,” *Optical Microlithography XI*, L. Van den Hove, ed., *Proceedings of SPIE* **3334**, p. 281 – 288, SPIE, Santa Clara, CA, 1998.
6. N. Farrar *et al.*, “Illuminator characterization using in–situ reticle diagnostic structures,” *Proceedings of INTERFACE ’99*, p. 85 – 96, Arch Chemicals, Inc., 1999.
7. Bevington, Philip R., *Data Reduction and Error Analysis for the Physical Sciences*, McGraw–Hill, New York, 1969.